Journal of Materials Chemistry B

Accepted Manuscript

ROYAL SOCIETY OF CHEMISTRY

www.rsc.org/materialsB

Journal Name

RSCPublishing

ARTICLE

Amphiphilic Trismethylpyridylporphyrin-Fullerene (C_{70}) Dyad: An Efficient Photosensitizer under Hypoxia Condition

Cite this: DOI: 10.1039/xoxxoooooox

Received ooth January 2012,
Accepted ooth January 2012

DOI: 10.1039/xoxxoooooox

www.rsc.org/

Mirong Guan,[a] Tingxiao Qin,[b] Jiechao Ge,[c]* Mingming Zhen,[a] Wei Xu,[a] Daiqin Chen,[a] Shumu Li,[a] Chunru Wang,[a] Hongmei Su,[b]* and Chunying Shu[a]*

Amphiphilic trismethylpyridylporphyrin-C_{70} (PC_{70}) dyad with improved photosensitization has been successfully prepared. The PC_{70} dyad forms liposomal nanostructure through molecular self-assembling. Increased absorption coefficient in visible region, good biocompatibility, and high photostability were observed on self-assembling structure. Surprisingly, in comparison with previously reported photosensitizer porphyrin, PC_{70} exhibited enhanced photodynamic therapy (PDT) effect under hypoxia condition. Further investigation illustrated that PC_{70} went through extremely long-life triplet state (211.3 μs) under hypoxia, which enabled the exiguous oxygen to approach and interact with the activated (^{3}P-C_{70})* more efficiently and produce more singlet oxygen. This would overcome the problems of existing photosensitizer as low PDT efficiency in cancerous tissue under hypoxia. The excellent properties of PC_{70} dyad would make it promising phototherapeutic agents especially for the treatment of early- and late-stage cancers under the shallow and hypoxia tissues.

Introduction

Photodynamic therapy (PDT) has recently attracted much attention because of its fine controllability, improved selectivity, and low systemic toxicity.[1] Photosensitizers (PSs) as PDT agents could react with oxygen in tissues upon light irradiation to generate reactive oxygen species (ROS), which is highly toxic to tumor cells.[2] However, current applications of PDT agents such as hematoporphyrin,[3] 5-Aminolevulinic acid (5-ALA),[4] tin ethyl etiopurpurin ($SnET_2$),[5] mono-L-aspartylchlorin e6 (Npe6),[6] are generally restricted by their drawbacks of poor solubility and photostability, low production of singlet oxygen ($^1O_2$) at tumor hypoxic microenvironment.[7] Therefore, it is still imperative to search the desired water-dispersible, highly photostable and efficient PDT agents, especially with high activity and biocompatibility under hypoxia tumor microenvironment.

Fullerene based nanomaterial has been applied in many areas, such as photoelectric device,[8] solar cells,[9] and MRI contrast agents.[10] Furthermore, a new application of fullerene derivatives as excellent PS for PDT[11] was under studied due to its unique properties including good biocompatibility, facile multiple surface functionalization, efficient generation of ROS under visible light illumination and total metabolism from living organism.[12] Very recently, we reported a carboxylic acid functionalized fullerene which exhibited excellent PDT property under white-light illumination.[13] As we know, the photodynamic activity of fullerenes can be further enhanced by conjugation with dye molecules[14] (e.g. porphyrin or phthalocyanine, which are standards of traditional PSs and have a natural proclivity to accumulate in cancer tissues.[15] Notably, activity of most PDT agents based on the concentration of the oxygen in the tissues,[16] while the hypoxic tumor microenvironment with low oxygen level brought down the PDT efficiency of these PSs. Viviana Rivarola's group reported a PS (porphyrin-C_{60}) that could produce singlet oxygen under anaerobic condition, however, the synthesized porphyrin-C_{60} exhibited poor solubility and further formulation process with liposome was required for application.[17]

Herein, we prepared an amphiphilic photosensitizer, trismethylpyridylporphyrin-C_{70} (PC_{70}) dyad, which could form a ring structure like liposome by self-assemble. The as-prepared PC_{70} showed enhanced absorption cross-section in visible region, good water-dispersibility, high photostability, and favorable biocompatibility. Significantly, the present PC_{70} exhibited extraordinary photodynamic effect even under hypoxic condition upon light irradiation. These excellent properties enable PC_{70} function as an improved PDT agent at low level of oxygen. Moreover, a possible mechanism has been proposed by investigating the transient absorption spectroscopy of PC_{70} according to laser flash photolysis.

Results and discussion

Characterization of PC_{70} and D-TMPyP

D-TMPyP was prepared according to established procedure,[18] and the synthetic route of D-TMPyP was outlined in Scheme S1 (SI). D-TMPyP reacted with C_{70} through one step reaction to achieve C_{70}-TMPyP according to our previously reported method.[19] After purification by flash chromatography, the chemical structure of products were confirmed by ^{1}H NMR

(DMSO-d_6) and MALDI-TOF-MS (α-cyano-4-hydroxy cinnamic acid as the matrix) (Fig.S1-S7). The obtained final product was mixed with methyl tosylate and refluxed in argon atmosphere and then passed through an anion-exchange resin repeatedly to yield Trismethylpyridylporphyrin-C_{70} as a chloride salt (PC_{70}). The absorption of PC_{70} and D-TMPyP were investigated (Fig. 1A). The molar absorption coefficient of Soret band of PC_{70} was less than that of D-TMPyP, and behaved a slightly red-shifted, which indicated that a partial of electron density migrated from the D-TMPyP ring to the fullerene entity. As a result, the prolonged lifetime of triplet of PC_{70} was observed as shown below. Fluorescence spectra were investigated in Fig S8-S9.[20] The fluorescence intensity of PC_{70} was decreased compared to D-TMPyP which indicated the interaction between D-TMPyP and C_{70}. Under irradiation of white light at 17 mW·cm^{-2} for 10, 30, 60, 90, 120 or 150 min, the absorbance intensity of PC_{70} decreased slowly, while that of both D-TMPyP and PpIX decreased dramatically (Fig. 1B). The result indicated that PC_{70} possessed better photostability than D-TMPyP and PpIX. In addition, the $^1O_2$ quantum yield of the PC_{70} was measured to be ca. 42% at white light (Fig. S10) with Rose Bengal as a standard photosensitizer.

The diameters of the D-TMPyP and PC_{70} were measured by dynamic light scattering (Nano-ZS ZEN3600, Malvern Instruments, Germany). Hydrodynamic size of PC_{70} (ca. 90 nm) is smaller than that of D-TMPyP (ca. 220 nm) (Fig. 1C). This size would facilitate the PC_{70} to be taken up by cells. In addition, zeta potentials (ζ) of PC_{70} and D-TMPyP were also measured (Fig. 1D). Only minute difference of ζ-potential of D-TMPyP and PC_{70} was observed. The appropriate size and zeta potential may lead to cellular uptake toward nanoparticles more easily.[21]

Most interestingly, the self-assembling of amphiphilic PC_{70} forms a ring circle structure similar to liposome, which was identified by transmission electron microscope (Fig. S11). The formed assembling structure exhibits diameter ca. 30 nm and may be further developed for drug delivery.

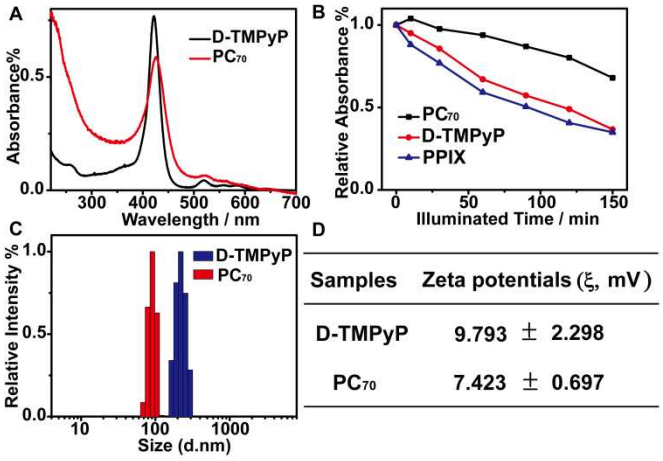

Fig. 1 (A) UV-Vis absorption Spectra of PC_{70} and D-TMPyP in water; (B) The relative absorbance of PC_{70}, D-TMPyP and PpIX exposed to light irradiation for 10, 30, 60, 90, 120 and 150 min, respectively, at a power density of 17 mW·cm^{-2}; (C) Size distribution of PC_{70} and D-TMPyP; (D) Zeta potential of PC_{70} and D-TMPyP (pH = 7.4).

Comparison of Cellular Uptake of PC_{70} and D-TMPyP

The cellular uptake of sensitizer was evaluated by incubating 10 μM of PC_{70} with A549 cells at various time points.[17] The uptake of D-TMPyP by A549 cells was parallel tested as control group. In each case, the concentration of intracellular sensitizer was measured by UV-Vis absorption. PC_{70} was rapidly internalized into A549 cells in 3 h and reached a plateau after incubation for 8 h (Fig. 2A). The maximum uptake value of PC_{70} (~20 nmol·10^{-6} cells) was three fold of that of D-TMPyP. This is due to the amphipathic property of PC_{70} that make it more easily across the cytomembrane.

Another experiment was explored to study the mechanism of cellular uptake of PC_{70} nanoparticles by incubating the A549 cells with PC_{70} and ionic D-TMPyP at 4°C and 37°C, respectively. The result was shown in Fig. 2B, both PC_{70} and D-TMPyP showed more cell uptaken at 37°C rather than 4°C. It was suggested that the cellular uptake of PC_{70} and D-TMPyP nanoparticles was energy-dependent.[22] In particularly, PC_{70} and D-TMPyP showed a selective uptake toward A549 cells in comparison with HaCaT cells (Fig. 2C), which may contribute to the tumor-targeting of D-TMPyP moiety.[23]

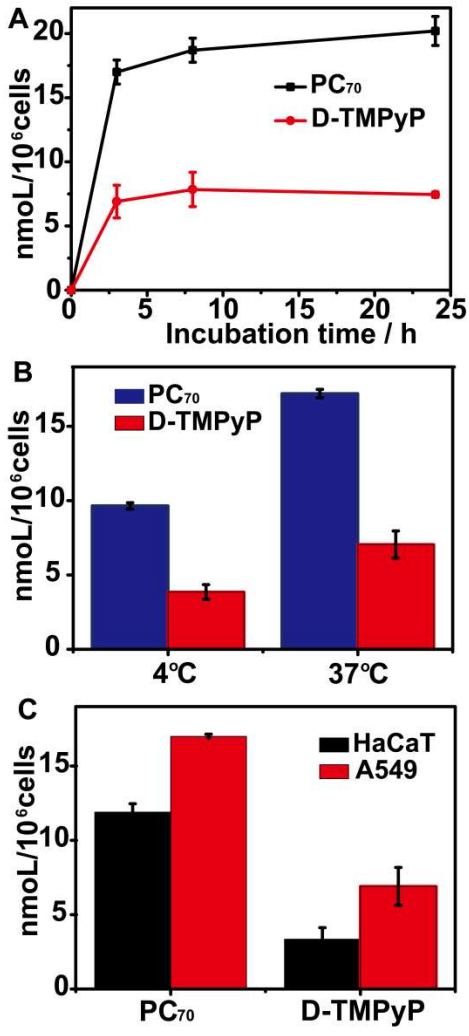

Fig. 2 (A) The comparison of uptake of PC_{70} and D-TMPyP into A549 cells at different incubation time; (B) Comparison of uptake of PC_{70} and D-TMPyP for 3 h incubation at 4°C and 37°C; (C) The comparison of uptake of PC_{70} and D-TMPyP into A549 cells and HaCaT cells, respectively. Values represent mean ± S.D. of three separated experiments.

Intracellular Location study of PC_{70} in A549 cells

To confirm that PC_{70} was internalized into cells, the localization of PC_{70} in A549 cells was characterized by laser scanning confocal microscopy, and D-TMPyP was used as a control. Both of PC_{70} and D-TMPyP emit red fluorescence upon excitation at 405 nm. As shown in Fig. 3A, the red fluorescence was distributed in most of cytoplasm which indicated that PC_{70} mainly located in cytoplasm but not nonspecifically attached to the cell membrane. Whereas, red fluorescence of D-TMPyP significantly quenched (Fig. 3B) indicated that little D-TMPyP molecules were uptaken by A549 cells. This result coincided with the previously reported. For further confirmation, transmission electron microscopy (H-7650 TEM Hitachi Ltd., Japan) was carried out to characterize the intracellular distribution of PC_{70}. As shown in Fig. 3D, PC_{70} (indicated by white arrows) was phagocytized into cell as a small cluster and mostly localized in the cytoplasm. In contrast, the control without treated with PC_{70} didn't show any nanoparticles (Fig. 3C). The favorable uptake toward cancerous cells of PC_{70} would facilitate its PDT efficiency.

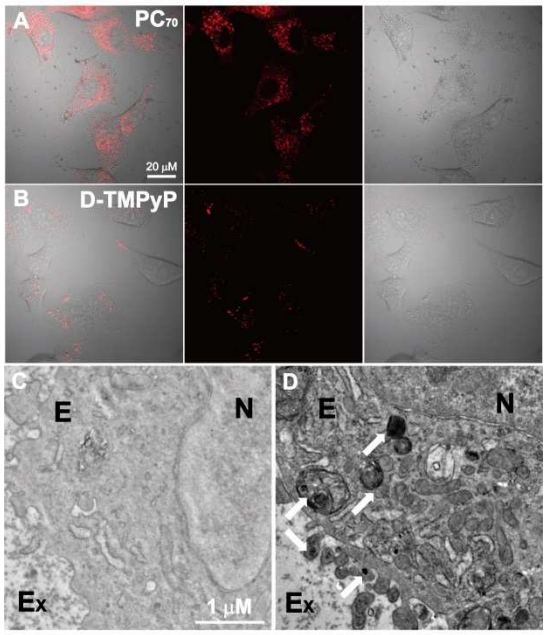

Fig. 3 (A) Confocal images of PC_{70} uptake into A549 cells after 3 h incubation; (B) Confocal images of D-TMPyP treated under the same condition; the images of (A) and (B) from left to right represent merged fluorescence and optical images, fluorescence images and optical images, respectively. (C) TEM image of A549 cells without treatment of PC_{70}; (D) TEM image of A549 cells incubated with PC_{70}. N = nuclear region, E = endosome, Ex = extracellular region.

The Photodynamic Activity of PC_{70} under Air Condition

According to the cellular uptake results, PC_{70} was internalized into cells after incubation for 3 h. When upon light irradiation, PC_{70} with extended π-conjugated system facilitated visible light absorption in the range from 400 to 700 nm, and produced ROS to kill cells. Importantly, the dark cytotoxicity of PC_{70} was negligible for both cancer cells and normal cells, indicating the favorable biocompatibility of PC_{70} (Fig. 4A). To investigate the photodynamic activity of PC_{70} against cancer cell, we studied the viability of A549 cells *in vitro*. After exposure to white light for 5 min, 10 min and 20 min at a power density of 17 $mW \cdot cm^{-2}$, the cellular viability was detected. The result indicated that both of PC_{70} and D-TMPyP (Fig. S12) showed strong inhibitory effects on cell viability even at low concentration of 1 μM under light irradiation (Fig. 4B), the killing efficiency can reach 98%. As we expect, cellular toxicity could be improved by extending the irradiation time and increasing the PC_{70} concentration (Fig. 4C). That's to say, the photodynamic activity of the PC_{70} was dose- and irradiation time-dependent. Interestingly, the cell death was accompanied by membrane bleb. As shown in Fig. 4D, blebs appeared on several cells after irradiation for 1 min. During irradiation last for 5 min, blebs appeared on most of cellular membranes, and blebs appeared on nuclear membranes after irradiation for 10 min (Fig. S13). This results was similar to our previous reported.[13a]

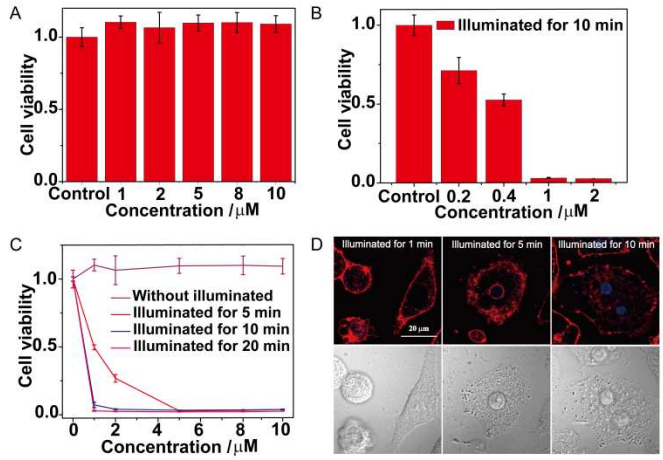

Fig. 4 (A) Cell viability of A549 cells incubated with different concentrations of PC_{70} for 24 h in dark; (B) Cell viability of A549 cells incubated with PC_{70} at gradient concentrations for 3 h and exposed to light irradiation for 10 min at a power density of 17 $mW \cdot cm^{-2}$; (C) Dose- and time- dependent PDT effects of PC_{70} on the A549 cell viability; (D) Confocal images of A549 cells stained with Dil and Hoechst 33258 after treated with 2 μM of PC_{70} for 3 h and exposed to light irradiation for 1, 5 and 10 min, respectively. The above images represent fluorescence images and those at bottom represent optical images. Values represent mean ± S.D. of three separated experiments.

The Photodynamic Activity of PC_{70} under Nitrogen Condition

Most of PDT efficiency relies on the concentration of oxygen around the tumor tissues, however, the tumor microenvironment is usually hypoxic and acidic.[24] As a result, the hypoxic tumor microenvironment significantly hindered the efficiency of the PDT. In order to illustrate thoroughly the PDT efficiency of PC_{70} under hypoxia, we further investigated the PDT efficiency of PC_{70} under anaerobic condition with white light irradiation. After incubating with either PC_{70} or D-TMPyP, A549 cells were exposed to light under nitrogen atomosphere. As shown in Fig. 5A, A549 cells in the presence of PC_{70} showed a severe photodamage (80%), in contrast, D-TMPyP only showed limited damage (22%) to A549 cells. This result demonstrated that the PDT efficiency of PC_{70} was higher than that of D-TMPyP in hypoxic environment. Furthermore, confocal microscopy experiment was carried out. When the A549 cells were incubated with PC_{70}, PI stained the cell nucleus transmembrane with red fluorescence, demonstrating that the cells damage severely (Fig. 5B). Meanwhile, most of A549 cells treated with D-TMPyP were not stained by PI, indicating that D-TMPyP didn't show significant cytotoxicity to A549 cells under the anaerobic condition. The remarkable

cytotoxicity of PC_{70} to tumor cells makes it potential as an excellent photosensitizer, especially under anaerobic condition.

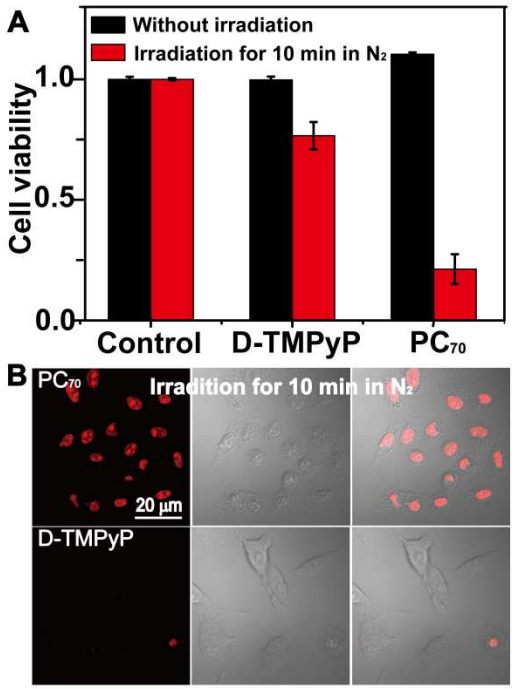

Fig. 5 (A) The comparison of Cell viability of A549 cells incubated with either PC_{70} or D-TMPyP for 3 h and subsequent irradiation for 10 min at a power density of 17 $mW \cdot cm^{-2}$ in nitrogen atmosphere. Cells without irradiation were used as a control. (B) Confocal images of A549 cells stained with PI after treated with 2 μM PC_{70} for 3 h and subsequently exposed to light irradiation for 10 min at a power density of 17 $mW \cdot cm^{-2}$ in nitrogen atmosphere. Cells treated with D-TMPyP were used as a control. Values represent mean ± S.D. of three separated experiments.

Mechanistic Study of Super Photodynamic Activity under Nitrogen Condition

In order to understand why PC_{70} is more effective to kill cells than D-TMPyP under nitrogen condition, a series of experiments were carried out. Free radical species detection was executed to identify which kind of ROS was produced by PC_{70} under light irradiation at the presence of different ROS scavenger.[25] A549 cells were incubated with PC_{70} (2 μM) in dark for 3 h, then the medium were replaced by DMEM without phenol red containing either 10 mM sodium azide (NaN_3), or mannitol, or SOD (50 units). Then cells were irradiated under white light for 10 min. The results in Fig. 6A and 6B indicated that both of PC_{70} and D-TMPyP induced cell death as a result of the generation of $^1O_2$ under air condition. The photo irradiation experiments at presence of different ROS scavenger were also carried out under nitrogen condition. The results were similar to that of under air-saturated conditions (Fig. 6C and 6D). Cells incubation with NaN_3, mannitol, and SOD were used as control (Fig. S14).

To quantify the photosensitizing ability of PC_{70} and D-TMPyP in producing singlet oxygen, the electron spin-resonance (ESR) spectroscopy was measured under air condition and nitrogen condition. 2,2,6,6-Tetramethylpiperidin (TEMP) was used as a radical scavenger.[26] As shown in Fig. S15A and S15B, under air condition little difference of PC_{70} and D-TMPyP was observed. However, after purging with nitrogen for 20 min, the ESR intensity treated with PC_{70} is reduced to half of the original. Meanwhile, that treated with D-TMPyP nearly disappeared (Fig. S15C and S15D), suggesting that the PC_{70} produce ROS at lower oxygen level more efficiently than D-TMPyP under hypoxic condition.

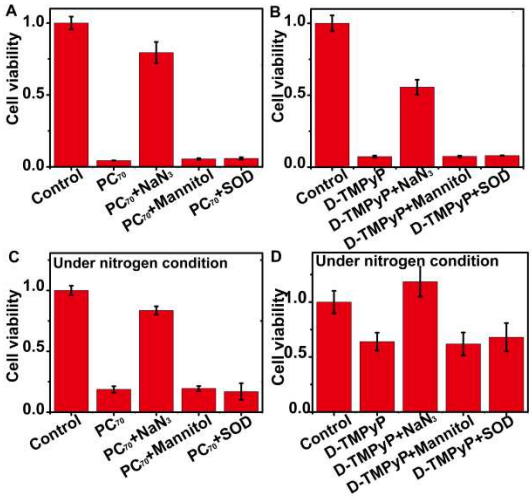

Fig. 6 (A) Viability of A549 cells incubated with 2 μM PC_{70} for 3 h in presence of different ROS quenchers upon light irradiation for 10 min. (B) Viability of A549 cells incubated with 2 μM of D-TMPyP for 3 h in presence of different ROS quenchers upon light irradiation for 10 min. (C) Viability of A549 cells incubated with 2 μM PC_{70} for 3 h in presence of different ROS quenchers upon light irradiation for 10 min under nitrogen condition. (D) Viability of A549 cells incubated with 2 μM D-TMPyP for 3 h in presence of different ROS quenchers upon light irradiation for 10 min under nitrogen condition. Values represent mean ± S.D. of three separated experiments.

The transient absorption spectroscopy based on laser flash photolysis was applied to detect the triplet excited state lifetime of D-TMPyP and PC_{70}, which was associated with the photosensitizing efficiency of D-TMPyP and PC_{70} in producing singlet oxygen. As shown in Fig. 7, the temporal decay for the triplet absorption band at 480 nm was monitored.[27] Under air-saturated condition, as shown in Fig. 7A, the triplet lifetime of PC_{70} (1.86 μs ± 0.01 μs) was slightly longer than that of D-TMPyP (1.64 μs ± 0.01 μs) under air-saturated condition. So there is no significant difference on the behavior of cell damage between PC_{70} and D-TMPyP under air-saturated condition. However, under N_2-saturated condition, distinctive triplet decay behavior was exhibited for PC_{70} and D-TMPyP, as shown in Fig. 7B. Unlike D-TMPyP triplet which had a single-exponential decay lifetime of 71.3 μs ± 0.5 μs, the PC_{70} triplet followed a second-order exponential decay with lifetime of 62.8 μs ± 4.8 μs (32%) and 211.3 μs ± 7.0 μs (68%). The relaxation pathways of PC_{70} triplet state, as illustrated in Fig. 7C, can reasonably explain the double-exponential result. The shorter lifetime of 62.8 μs, which was similar to 71.3 μs of D-TMPyP, was assigned to the decay of triplet state itself. In contrast, the longer lifetime of 211.3 μs can be assigned to the exciplex formed by energy transfer between excited D-TMPyP and ground state C_{70}. The formation of exciplex may be due to the longer lifetime of triplet which has larger probability formed at low oxygen concentration. It was the formation of exciplex that increased the triplet lifetime of PC_{70}. Under low oxygen concentration condition, the diffusion rate of oxygen

was low, the elongated triplet lifetime of PC_{70} made it still possible to photosensitize the ground state of oxygen to produce singlet oxygen, whereas the shorter-lived triplet state of D-TMPyP had much less efficiency in photosensitization. This could explain why PC_{70} retains PDT ability to kill cells under low oxygen concentration condition.

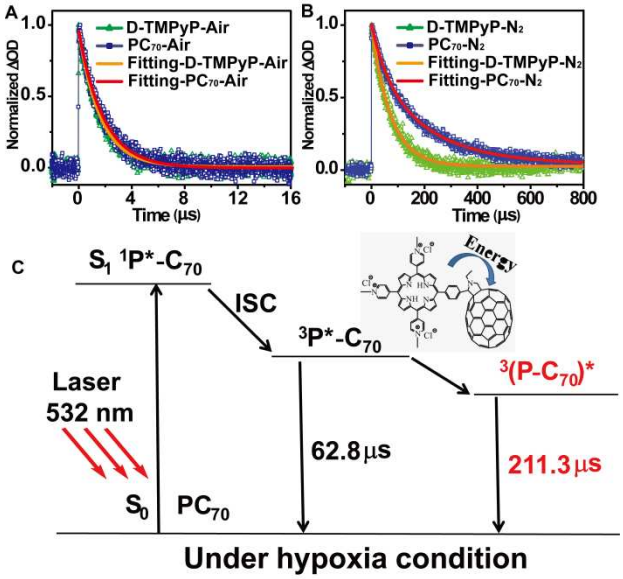

Fig. 7 The transient UV-visible absorption spectroscopies of D-TMPyP and PC_{70} under different conditions. (A) Under air-saturated condition and (B) Under N_2-saturated condition. (C) The illustrated relaxation pathways of PC_{70} triplet state.

Conclusions

In conclusion, the successfully synthesized photosensitizer (PC_{70}) based on trismethylpyridylporphyrin-C_{70} dyad was investigated. The as-prepared PC_{70} performed good water dispersibility, high photostability, and favorable biocompatibility. Significantly, the present PC_{70} exhibits extraordinary photodynamic effects even under the hypoxia condition upon light irradiation. These excellent properties enable PC_{70} facilitate the PDT of cells with lower level of oxygen. Further investigation illustrated that PC_{70} possessed extremely long-life triplet state (211.3 μs) under hypoxia condition, which enabled the exiguous oxygen had enough diffusion time to reach the activated (^{3}P-C_{70})* and interacted with each other to produce singlet state oxygen. This find may make PC_{70} promising as an improved PDT agent and especially can be used in the treatment of early- and late-stage cancers under shallow and hypoxia tissues.

Experimental section

Preparation and Characterization of the water-soluble PC_{70} and the water-soluble Trismethylpyridylporphyrin

Experimental details of the synthetic procedures and analysis of characterization are given in the Supporting Information.

$^1O_2$ quantum yield measurement via a chemical method.[28]

Water soluble disodium 9, 10-anthracendipropionic acid (Na_2-ADPA) was used as a $^1O_2$ trapping agent, and Rose Bengal (RB) was used as a standard photosensitizer. In the experiment, 100 μL of Na_2-ADPA solution (1 mg/mL) was added into 1.5 mL of PC_{70} solution. The resulting solution was irradiated under white light (400-700 nm) at a power density of 10 mW/cm^2. To eliminate the inner-filter effect, the absorption maxima of RB and PC_{70} were adjusted to about 0.2 OD. The absorption of Na_2-ADPA at 380 nm was recorded at different irradiation time to get the decay rate of photosensitizing process. The $^1O_2$ quantum yield of PC_{70} in water (ΦPC_{70}) was calculated using the formula below.

$$\Phi PC_{70} = \Phi RB \times KPC_{70} \times ARB/(KRB \times APC_{70})$$

Where, KPC_{70} and KRB are the decomposition rate constants of Na_2-ADPA by PC_{70} and RB, respectively. APC_{70} and ARB represent light absorption by PC_{70} and the RB, respectively, which are determined by integration of the optical absorption bands in the wavelength range 400-700 nm. ΦRB is the $^1O_2$ quantum yield of RB, and ΦRB = 75% in water. The measured $^1O_2$ quantum yield of PC_{70} in water is ca. 42%.

Cell Culture

The A549 cells and HaCaT cells were cultured with Dulbecco's modified Eagle's medium (DMEM) (Invitrogen, USA) supplemented with 10% fetal bovine serum (Hyclone Company, South Logan, UT), penicillin (100 μg·mL^{-1}), and streptomycin (100 μg·mL^{-1}) (Gibco, Grand Island, N. Y. USA) in 5% CO_2 at 37^{o}C in a humidified incubator.

Assays of cellular uptake of PC_{70} and D-TMPyP

As mentioned above, an appropriate number of A549 cells (ca. 5×10^5 cells·cm^{-2}) were incubated with PC_{70} (10 μM) in the culture flasks at different incubation time points, such as 3 h, 8 h and 24 h in dark at 37^{o}C. Then the culture medium was removed and the cells were washed several times with icy PBS solution. The cellular uptake was determined by adding 1.0 mL of 4% sodium dodecyl sulphate (SDS, Merck) to the culture flasks and subsequent incubating for 15 min in the dark at room temperature. The concentration of PC_{70} was evaluated by measuring the UV-vis absorbance at 428 nm. The concentration of D-TMPyP was examined under the same conditions but measured the UV-vis absorbance at 422 nm. Each experiment was compared with a culture control without photosensitizer. The same experiment was carried out to compare the cellular uptake of PC_{70} toward A549 cells and HaCaT cells through incubating 3 h in dark at 4^{o}C.

TEM Observation

A549 cells incubated with PC_{70} (2 μM) for 3 h and washed with Hank's balanced salt solution (HBSS) to remove the noninternalized nanoparticles. The obtained cells were fixed with 4% glutaraldehyde and 4% paraformaldehyde overnight at 4^{o}C respectively. After that, cells were centrifuged at 1000 rpm for 3 min, and washed with PBS (1 mM) for three times. Afterwards the cells were post-fixed in 1% osmium tetraoxide for 2 h at room temperature in 1 mm^3 masses. After dehydrated by a graded series of ethanol and acetone the cells were embedded in Epon812. Ultramicrotome (UC6, Leica Ltd. Co, Germany) were used to cut ultrathin sections and transferred onto 200-mesh copper grids, which were stained with uranyl acetate and lead nitrate, then observed with a H-7650 TEM instrument (Hitachi Ltd., Japan).

PDT treatment and cell viability assay

Before cultured in 96-well plate for 24 h, cells were counted using a cell counter to control the cell density at ca. 5×10^4 cells·cm^{-2}, and then incubated with PC_{70} for 3 h in dark at 37^{o}C.

After removing the culture medium, DMEM was added into the plate. The cells were subsequently irradiated with the M-visual light source (MVL-210, MEJIRO GENOSSEN, Japan) at 17 $mW \cdot cm^{-2}$ for 10 minutes. Then fresh culture medium was added to replace the aged one and cultivated the cells for 24 h in the dark at 37°C. The same procedure without irradiation was carried out to determine the dark toxicity. Cytotoxicity was evaluated by a WST-8 assay with a Cell counting Kit-8 (CCK-8; DOJINDO, Kumamoto, Japan) which has characteristic absorbance at 450 nm. This can be read with a 96-well plate reader (iMarkmicroplate reader, Bio-RAD, USA) to determine the cell viability. During the experiment, the D-TMPyP was used as a control.

Confocal images after staining with Dil and Hoechst 33258

First, A549 cells were incubated with different concentration of PC_{70} and D-TMPyP at 37°C, 5% CO_2 for 3 h, respectively. Then aged cell culture was replaced with fresh DMEM (without phenol red) and exposed to white light for 1 min, 5 min and 10 min, respectively, at a power density of 17 $mW \cdot cm^{-2}$, the cellular viability was detected. After that, either Hoechst 33258 (1 $mg \cdot mL^{-1}$) or Dil (1 $mg \cdot mL^{-1}$) was added and incubated with the cells for 20 min before observation. The image was obtained by a FV 1000-IX81 confocal laser scanning microscope (Olympus, Japan).

Inhibition of ROS Generation

A549 cells with a cell density of ca. 5×10^4 $cells \cdot cm^{-2}$ were cultured in a 96-well plate for 24 h. To inhibit the ROS generation, A549 cells were incubated with PC_{70} (2 μM) in dark for 3 h, then the aged medium was replaced by fresh medium containing either 10 mM sodium azide (NaN_3), or mannitol, or SOD (50 units) and cells were irradiated under white light for 10 min. After that, the medium containing free-radical scavenger was replaced. 1 day later, the cell viability was detected by CCK-8. Under the same conditions, several ROS scavenger (NaN_3, singlet oxygen ($^1O_2$) quencher, mannitol, a hydroxyl radical ($^{\cdot}OH$) quencher, and superoxide dismutase (SOD), a superoxide anion free radical ($O_2^{\cdot -}$) quencher) were used as controls.

Evaluation of radical scavenging ability by ESR spectroscopy:

Studies on radical scavenging by PC_{70} (10 μM) were performed by spin trapping of 2,2,6,6-Tetramethylpiperidin (TEMP). ESR spectra were measured with a Bruker ELEXSYSE 500 ESR spectrometer at 25°C. Singlet oxygen was generated from light irradiation (50 mW/cm^2). D-TMPyP (10 μM) was used as a control. After purging with nitrogen for 20 min, the ESR intensity of TEMP containing either PC_{70} or D-TMPyP was also detected.

PDT treatment under anaerobic condition

A549 cells were incubated with either PC_{70} (2 μM) or D-TMPyP (2 μM) in dark for 3 h at 37°C as previously described but in nitrogen atmosphere, and then exposed to light irradiation for 10 min. The medium was replaced by the fresh DMEM (without phenol red). Cell viability was detected by CCK-8 after one day incubiation. After removing the medium and washing by PBS for several times. The cells were stained with propidium iodide (PI) (8 μM) for 15 min before observation. The images were obtained by n FV 1000-IX81 confocal laser scanning microscope (Olympus, Japan).

Acknowledgements

This work is supported by the National Natural Science Foundation of China (Nos. 31170963, 51372251) and the Key Research Program of the Chinese Academy of Sciences (Grant No. KGZD-EW-T02).

Notes and references

[a]Key Laboratory of Molecular Nanostructure and Nanotechnology, Institute of Chemistry, Chinese Academy of Sciences, and Beijing National Laboratory for Molecular Sciences, Beijing 100190, China. E-mail: shucy@iccas.ac.cn

[b]Beijing National Laboratory for Molecular Sciences (BNLMS), State Key Laboratory of Molecular Reaction Dynamics, Institute of Chemistry, Chinese Academy of Sciences, Beijing 100190, P. R. China.

[c]Key Laboratory of Photochemical Conversion and Optoelectronic Materials, Technical Institute of Physics and Chemistry (TIPC), Chinese Academy of Sciences, Beijing, 100190, China.

† Supplementary information See DOI:10.1039/b000000x/

1 a) D. Dolmans, D. Fukumura, R. Jain, *Nat. Rev. Cancer* 2003, **3**, 380; b) F. Schmitt, J. Freudenreich, N. Barry, L. Juillerat-Jeanneret, G. Suss-Fink, B. Therrien, *J. Am. Chem. Soc*., 2012, **134**, 754; c) Y. Cakmak, S. Kolemen, S. Duman, Y. Dede, Y. Dolen, B. Kilic, Z. Kostereli, L. Yildirim, A. Dogan, D. Guc, E. Akkaya, *Angew. Chem. Int. Ed.,* 2011, **50**, 11937; d) J. Barreto, W. O'Malley, M. Kubeil, B. Graham, H. Stephan, L. Spiccia, *Adv. Mater.,* 2011, **23**, H18; e) J. Celli, B. Spring, I. Rizvi, C. Evans, K. Samkoe, S. Verma, B. Pogue, T. Hasan, *Chem. Rev.,* 2010, **110**, 2795; f) L. Li, M. Nurunnabi, M. Nafiujjaman, Y. Jeong, Y. Lee, K. Huh, *J. Mater. Chem. B,* 2014, **2**, 2929.

2 a) Z. Zhu, Z. Tang, J. Phillips, R. Yang, H. Wang, W. Tan, *J. Am. Chem. Soc.,* 2008, **130**, 10856; b) E. Shibu, S. Sugino, K. Ono, H. Saito, A. Nishioka, S. Yamamura, M. Sawada, Y. Nosaka, V. Biju, *Angew. Chem. Inter. Ed.,* 2013, **52**, 10559; c) C. Schweitzer, R. Schmidt, *Chem. Rev.,* 2003, **103**, 1685; d) S. Jin, L. Zhou, Z. Gu, G. Tian, L. Yan, W. Ren, W. Yin, X. Liu, X. Zhang, Z. Hu, Y. Zhao, *Nanoscale*, 2013, **5**, 11910; e) H. Kim, S. Mun, Y. Choi, *J. Mater. Chem. B,* 2013, **1**, 429.

3 Y. Ren, R. Wang, Y. Liu, H. Guo, X. Zhou, X. Yuan, C. Liu, J. Tian, H. Yin, Y. Wang, *Biomaterials,* 2014, **35**, 2462.

4 a) G. Berkovitch, D. Doron, A. Nudelman, Z. Malik, A. Rephaeli, *J. Med. Chem.,* 2008, **51**, 7356; b) F. Giuntini, L. Bourre, A. MacRobert, M. Wilson, I. Eggleston, *J. Med. Chem.,* 2009, **52**, 4026.

5 M. Kaplan, R. Somers, R. Greenberg, et al. *J. Surg. Oncol.,* 1998, **67**, 121.

6 a) A. Chan,; M. Juarez, R. Allen, W. Volz, T. Albertson, *Photodermatol. Photo.,* 2005, **21**, 72; b) S. Taber, V. Fingar, C. Coots, T. Wieman, Clin. *Cancer Res.,* 1998, **4**, 2741.

7 a) S. Wang, P. Huang, L. Nie, R. Xing, D. Liu, Z. Wang, J. Lin, S. Chen, G. Niu, G. Lu, X. Chen, *Adv. Mater.,* 2013, **25**, 3055; b) S. Walenta, M. Wetterling, M. Lehrke, G. Schwickert, K. Sundfor, E. Rofstad, W. Mueller-Klieser, *Cancer Res.*, 2000, **60**, 916.

8 a) H. Li, B. Tee, J. Cha, Y. Cui, J. Chung, S. Lee, Z. Bao, *J. Am. Chem. Soc.,* 2012, **134**, 2760; b) S. Sato, H. Nikawa, S. Seki, L.

Wang, G. Luo, J. Lu, M. Haranaka, T. Tsuchiya, S. Nagase, T. Akasaka, *Angew. Chem. Int. Ed.* 2012, **51**, 1589.

9 a) X. Meng, W. Zhang, Z. Tan, Y. Li, Y. Ma, T. Wang, L. Jiang, C. Shu, C. Wang, *Adv. Funct. Mater.*, 2012, **22**, 2187; b) X. Meng, G. Zhao, Q. Xu, Z. Tan, Z. Zhang, L. Jiang, C. Shu, C. Wang, Y. Li, *Adv. Funct. Mater.*, 2014, **24**, 158.

10 a) C. Shu, C. Wang, J. Zhang, H. Gibson, H. Dorn, F. Corwin, P. Fatouros, T. Dennis, *Chem. Mater.,* 2008, **20**, 2106; b) R. Bolskar, A. Benedetto, L. Husebo, R. Price, E. Jackson, S. Wallace, L. Wilson, J. Alford, *J. Am. Chem. Soc.,* 2003, **125**, 5471.

11 a) J. Fan, G Fang, F. Zeng, X. Wang, S. Wu, *Small*, 2013, **9**, 613; b) R. Mendes, A. Bachmatiuk, B. Buchner, G. Cunibertib, M. Rummeli, *J. Mater. Chem. B,* 2013, **1**, 401; c) W. Jang, D. Yim, I. Hwang, *J. Mater. Chem. B*, 2014, **2**, 2202; d) Y. Yamakoshi, N. Umezawa, A. Ryu, K. Arakane, N. Miyata, Y. Goda, T. Masumizu, T. Nagano, *J. Am. Chem. Soc.* 2003, **125**, 12803; e) P. Padmawar, T. Canteenwala, S. Verma, L. Tan, G. He, P. Prasad, L. Chiang, *Chem. Mater.* 2006, **18**, 4065.

12 a) F. Giacalone, N. Martin, *Chem. Rev.* 2006, **106**, 5136; b) A. Ikeda, M. Akiyama, T. Ogawa, T. Takeya, *ACS Med. Chem. Lett.* 2010, **1**, 115; c) D. McCluskey, T. Smith, P. Madasu, C. Coumbe, M. Mackey, P. Fulmer, J. Wynne, S. Stevenson, J. Phillips, *ACS Appl. Mater. Interfaces*, 2009, **1**, 882; d) E. Otake, S. Sakuma, K. Torii, A. Maeda, H. Ohi, S. Yano, A. Morita, *Photochem. Photobiol.*, 2010, **86**, 1356; e) M. Wang, S. Maragani, L. Huang, S. Jeon, T. Canteenwala, M. Hamblin, L. Chiang, *Eur. J. Med. Chem.* 2013, **63**, 170; f) P. Mroz, A. Pawlak, M. Satti, H. Lee, T. Wharton, H. Gali, T. Sarna, M. Hamblin, *Free Radic. Biol. Med.* 2007, **43**, 711.

13 a) Q. Liu, M. Guan, L. Xu, C. Shu, C. Jin, J. Zheng, X. Fang, Y. Yang, C. Wang, *Small*, 2012, **8**, 2070; b) Q. Liu, L. Xu, X. Zhang, N. Li, J. Zheng, M. Guan, X. Fang, C. Wang, C. Shu, *Chem. Asian J.* 2013, **8**, 2370.

14 a) X. Liu, M. Zheng, X. Kong, Y. Zhang, Q. Zeng, Z. Sun, W. Buma, H. Zhang, *Chem. Commun*. 2013, **49**, 3224; b) X. Wang, C. Yang, J. Chen, X. Yan, *Anal.Chem.* 2014, **86**, 3263; c) G. He, L. Tan, Q. Zheng, P. Prasad, *Chem. Rev.,* 2008, **108**, 1245.

15 a) T. Dougherty, J. Kaufman, A. Goldfarb, K. Weishaupt, D. Boyle, A. Mittleman, *Cancer Res.* 1978, **38**, 2628; b) R. Lipson, A. Olsen, *J. Natl. Cancer Inst.* 1961, **26**, 1; c) T. Dougherty, G. Grinndey, R. Fiel, K. Weishaupt, D. Boyle, *J. Natl. Cancer Inst.* 1975, **55**, 115.

16 a) Q. Lin, C. Bao, Y. Yang, Q. Liang, D. Zhang, S. Cheng, L. Zhu, *Adv. Mater.* 2013, **25**, 1981; b) C. Jin, J. Lovell, J. Chen, G. Zheng, *ACS Nano.,* 2013, **7**, 2541; c) S. Wang, P. Huang, L. Nie, R. Xing, D. Liu, Z. Wang, J. Lin, S. Chen, G. Niu, G. Lu, X. Chen, *Adv. Mater.,* 2013, **25**, 3055.

17 M. Alvarez, C. Prucca, M. Milanesio, E. Durantini, V. Rivarola, *Int. J. Biochem. Cell Biol.,* 2006, **38**, 2092.

18 a), Y. Ishikawa, A. Yamashita, T. Uno, *Chem. Pharm. Bull.,* 2001,**49**, 287; b) K. Okuda, C. Abeta, T. Hirota, M. Mochizuki, T. Mashino, *Chem. Pharm. Bull.,* 2002, **50**, 985.

19 W. Xu, L. Feng, Y. Wu, T. Wang, J. Wu, J. Xiang, B. Li, L. Jiang, C. Shu, C. Wang, *Phys. Chem. Chem. Phys.* 2011, **13**, 428.

20 W. Lei, G. Jiang, Q. Zhou, Bao. Zhang and Xue. Wang, *Phys. Chem. Chem. Phys.* 2010, **12**, 13255.

21 M. Milanesio, M. Alvarez, J. Silber, V. Rivarola, E. Durantini, *Photochem. Photobiol.Sci.,* 2003, **2**, 926.

22 J. Li, F. Jiang, B. Yang, X. Song, Y. Liu, H. Yang, D. Cao, W. Shi, G. Chen, *Sci. Rep.,*2013, **3**, 1998.

23 a) P. Kubat, K. Lang, P. Anzenbacher, *Biochim. Biophys. Acta.,* 2004, **1670**, 40; b) Y. Shibata, A. Matsumura, F. Yoshida, T. Yamamoto, K. Nakai, T. Nose, I. Sakata, S. Nakajima, *Cancer Lett.*2001, **166**, 79; c) R. Song, Y. Kim, Y. Sohn, *J. Inorg. Biochem.* 2002, **89**, 83; d) A. Kano, Y. Taniwaki, I. Nakamura, N. Shimada, K. Moriyama, A. Maruyama, *J. Control Release* 2013, **167**, 315.

24 a) J. Brown, W. Wilson, *Nat. Rev. Cancer*, 2004, **4**, 437; b) X. Yue, C. Yanez, S. Yao, K. Belfield, *J. Am. Chem. Soc.,* 2013, **135**, 2112; c) P. Prasad, C. Gordijo, A. Abbasi, A. Maeda, A. Ip, A. Rauth, R. DaCosta, X. Wu, *ACS Nano.* 2014, **8**, 6510; d) N. Kong, K. Lin, H. Li, J. Chang, *J. Mater. Chem. B,* 2014, **2**, 1100.

25 a) S. Cherng, Q. Xia, L. Blankenship, J. Freeman, W. Wamer, P. Howard, P. Fu, Chem. Res. *Toxicol,* 2005, **18**, 129; b) R. Williams, T. Glinka, M. Flanagan, R. Gallegos, H. Coffman, D. Pei, *J. Am. Chem. Soc.,* 1992, **114**, 733; c) E. Rozhkova, I. Ulasov, B. Lai, N. Dimitrijevic, M. Lesniak, T. Rajh, *Nano. Lett.,* 2009, **9**, 3337; d) Y. Jin, J. Cowan, *J. Am. Chem. Soc.,* 2005, **127**, 8408; e) Q. An, C. Sun, D. Li, K. Xu, J. Guo, C. Wang, *ACS Appl. Mater. Interfaces*, 2013, **5**, 13248; f) S. Kruss, M. P. Landry, E. Vander Ende, B. Lima, N. Reuel, J. Zhang, J. Nelson, B. Mu, A. Hilmer, M. Strano, *J. Am. Chem. Soc.,*2014, **136**, 713.

26 a) W. He, H. Kim, W. Wamer, D. Melka, J. Callahan, J. Yin, *J. Am. Chem. Soc.* 2014, **136**, 750; b) W. Zhang, X. Gong, C. Liu, Y. Piao, Y. Sun, G. Diao, *J. Mater. Chem. B,* 2014, **2**, 5107.

27 a) C. Zhang, J. Zhao, S. Wu, Z. Wang, W. Wu, J. Ma, S. Guo, L. Huang, *J. Am. Chem. Soc.,* 2013, **135**, 10566; b) F. Deschler, A. Sio, E. Hauff, P. Kutka, T. Sauermann, H. Egelhaaf, J. Hauch, E. Como, *Adv. Funct. Mater.*, 2012, **22**, 1461.

28 J. Ge, M. Lan, B. Zhou, W. Liu, L. Guo, H. Wang, Q. Jia, G. Niu, X. Huang, H. Zhou, X. Meng, P. Wang, C. Lee, W. Zhang, X. Han, *Nat. Commun.,* 2014, **8**, 4596.

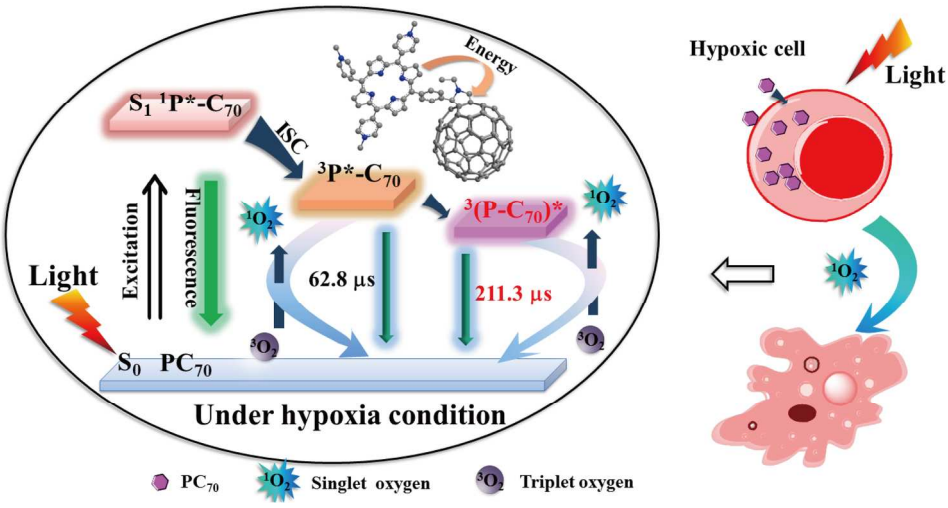

190x95mm (300 x 300 DPI)